HHS Public Access

Author manuscript

J Nat Prod. Author manuscript; available in PMC 2021 December 07.

Published in final edited form as:

J Nat Prod. 2021 May 28; 84(5): 1638–1648. doi:10.1021/acs.jnatprod.1c00179.

Grincamycins P–T: Rearranged Angucyclines from the Marine Sediment-Derived *Streptomyces* sp. CNZ-748 Inhibit Cell Lines of the Rare Cancer Pseudomyxoma Peritonei

Zhuo Shang[○],
Department of Chemistry and Biochemistry, University of South Carolina, Columbia, South Carolina 29208, United States

Zachary E. Ferris[○],
Department of Chemistry and Biochemistry, University of South Carolina, Columbia, South Carolina 29208, United States

Douglas Sweeney,
Center for Marine Biotechnology and Biomedicine, Scripps Institution of Oceanography, University of California San Diego, La Jolla, California 92093, United States

Alexander B. Chase,
Center for Marine Biotechnology and Biomedicine, Scripps Institution of Oceanography, University of California San Diego, La Jolla, California 92093, United States

Chunhua Yuan,
Nuclear Magnetic Resonance Facility, Campus Chemical Instrument Center, The Ohio State University, Columbus, Ohio 43210, United States

Yvonne Hui,
Department of Pathology, Microbiology and Immunology, School of Medicine, University of South Carolina, Columbia, South Carolina 29209, United States

Lukuan Hou,
Department of Chemistry and Biochemistry, University of South Carolina, Columbia, South Carolina 29208, United States

Ethan A. Older,
Department of Chemistry and Biochemistry, University of South Carolina, Columbia, South Carolina 29208, United States

Dan Xue,

Corresponding Author: **Jie Li** – Phone: +1 8037775010; LI439@mailbox.sc.edu.

○Author Contributions

Z.S. and Z.E.F. contributed equally to this work.

Supporting Information

The Supporting Information is available free of charge at https://pubs.acs.org/doi/10.1021/acs.jnatprod.1c00179.

Strain taxonomy of CNZ-748; BGC annotation; HPLC chromatogram of extract; UV, HRMS, and 1D and 2D NMR spectra of **1–9;** and cytotoxicity assay results (PDF)

Complete contact information is available at: https://pubs.acs.org/10.1021/acs.jnatprod.1c00179

The authors declare no competing financial interest.

Department of Chemistry and Biochemistry, University of South Carolina, Columbia, South Carolina 29208, United States

Xiaoyu Tang,
Institute of Chemical Biology, Shenzhen Bay Laboratory, Shenzhen 518132, China

Weipeng Zhang,
College of Marine Life Sciences, Ocean University of China, Qingdao 266100, China

Prakash Nagarkatti,
Department of Pathology, Microbiology and Immunology, School of Medicine, University of South Carolina, Columbia, South Carolina 29209, United States

Mitzi Nagarkatti,
Department of Pathology, Microbiology and Immunology, School of Medicine, University of South Carolina, Columbia, South Carolina 29209, United States

Traci L. Testerman,
Department of Pathology, Microbiology and Immunology, School of Medicine, University of South Carolina, Columbia, South Carolina 29209, United States

Paul R. Jensen,
Center for Marine Biotechnology and Biomedicine, Scripps Institution of Oceanography, University of California San Diego, La Jolla, California 92093, United States

Jie Li
Department of Chemistry and Biochemistry, University of South Carolina, Columbia, South Carolina 29208, United States

Abstract

While marine natural products have been investigated for anticancer drug discovery, they are barely screened against rare cancers. Thus, in our effort to discover potential drug leads against the rare cancer pseudomyxoma peritonei (PMP), which currently lacks effective drug treatments, we screened extracts of marine actinomycete bacteria against the PMP cell line ABX023-1. This effort led to the isolation of nine rearranged angucyclines from *Streptomyces* sp. CNZ-748, including five new analogues, namely, grincamycins P–T (**1–5**). The chemical structures of these compounds were unambiguously established based on spectroscopic and chemical analyses. Particularly, grincamycin R (**3**) possesses an *S*-containing α-L-methylthioaculose residue, which was discovered in nature for the first time. All of the isolated compounds were evaluated against four PMP cell lines and some exhibited low micromolar inhibitory activities. To identify a candidate biosynthetic gene cluster (BGC) encoding the grincamycins, we sequenced the genome of the producing strain, *Streptomyces* sp. CNZ-748, and compared the BGCs detected with those linked to the production of angucyclines with different aglycon structures.

Graphical Abstract

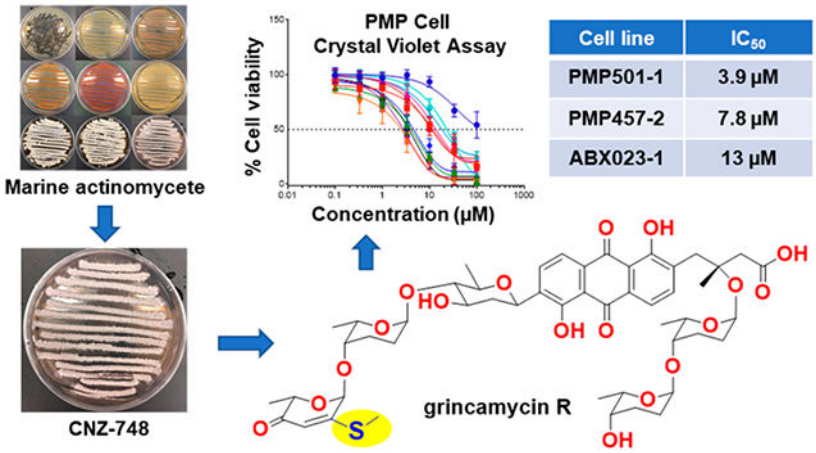

Marine actinomycete bacteria represent a prolific source for natural product (NP) drug discovery.[1] The structurally unique NPs produced by these marine microorganisms possess a variety of potent biological activities, particularly cytotoxic properties.[2,3] While cytotoxic activity has been a pursuit for marine-based NP drug discovery, NPs are seldom screened against cell lines of rare cancers, such as pseudomyxoma peritonei (PMP). PMP is a rare, highly mucinous appendiceal neoplasm that spreads to the peritoneal cavity, causing mucinous ascites and tumor implants on the surfaces of the peritoneal wall and abdominal organ surfaces.[4] PMP tumors tend to be poorly vascularized, and some exist as floating nodules. PMP can range from well differentiated, low-grade neoplasms with indolent growth to aggressive, poorly differentiated tumors with signet ring cell morphologies.[5] Because current chemotherapy drugs are rarely effective, the standard treatment for PMP is an intensive 8–14 h surgery that is a high risk for patients in poor health, leaving many patients without alternative treatment options.[6] Furthermore, ovarian, colorectal, and gastric cancers occasionally spread to the peritoneum and have the same need for improved treatments in these cases.[6]

Along with our collaborators, we are the first laboratory to have cultured PMP cell lines that can be passaged repeatedly (at least 20 times). This provides us a unique opportunity to screen marine microbial NPs for the discovery of potential leads against PMP. Thus, as an initial effort, extracts of 21 actinomycete strains isolated from marine sediment samples were screened *in vitro* against PMP cell lines. From the most potent extract, bioactivity-guided fractionation was performed, leading to the isolation of nine rearranged angucyclines, including five new analogues featuring unique structural modifications. These pure compounds exhibited mild to potent inhibitory activities against several different PMP cell lines.

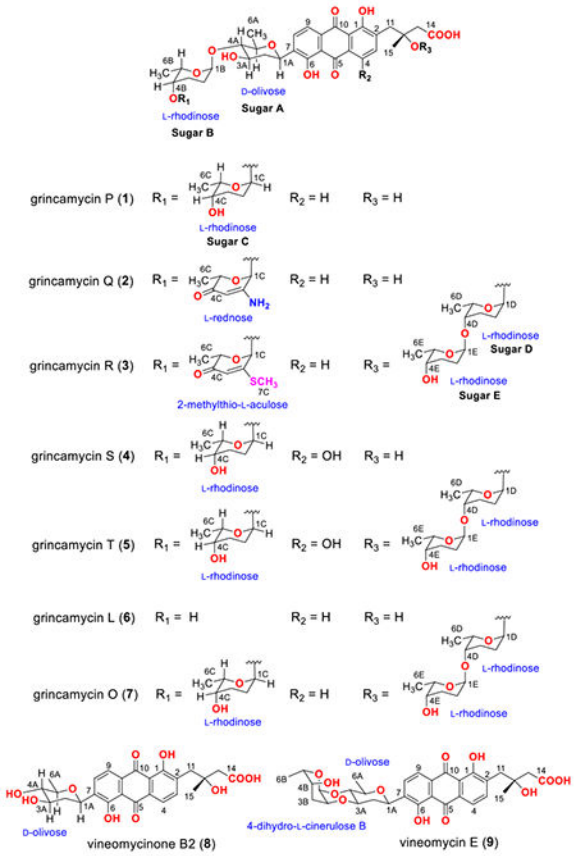

RESULTS AND DISCUSSION

In order to discover secondary metabolites from marine actinomycetes that inhibit PMP, we first screened *in vitro* inhibitory effects of EtOAc extracts of 21 actinomycete strains isolated from marine sediment samples using the PMP cell line ABX023-1, which originated from a tumor with signet ring cell morphology. One extract from the strain *Streptomyces* sp. CNZ-748 displayed inhibitory activity toward the PMP cell line ABX023-1, with an IC_{50} value of 40.5 μg/mL. To investigate the metabolite(s) responsible for the activity, we cultivated *Streptomyces* sp. CNZ-748 in A1 broth for 9 days at a 12 L scale (Figure S1). The EtOAc extract (1.6 g) of the bacterial broth was fractionated by reversed-phase C_{18} chromatography using a MeOH/H_2O gradient to afford 10 fractions. Each of these 10 fractions was tested against the same PMP cell line, with the fractions eluted by 70 and 80% MeOH/H_2O exhibiting IC_{50} values of 18.8 and 16.3 μg/mL, respectively. These fractions, guided by the PMP cell cytotoxicity assay, were successively fractionated via a Sephadex LH-20 column and semipreparative C_{18} HPLC chromatography to yield the active constituents, including five new rearranged angucyclines, grincamycins P–T (**1–5**), featuring new modifications on the terminal deoxy sugar moieties and anthraquinone aglycone, together with four known members of this structure class, grincamycin L (**6**), grincamycin O (**7**), vineomycinone B2 (**8**), and vineomycin E (**9**). In this report, we present a comprehensive study of 1–9, inclusive of detailed spectroscopic analysis and acid degradation leading to structure elucidation, the identification of a candidate biosynthetic

gene cluster (BGC) from the genome sequence, and inhibitory activities against cell lines of the rare cancer pseudomyxoma peritonei (PMP).

We first isolated grincamycin O (**7**), a major metabolite from the most active fraction (IC_{50} 16.3 μg/mL toward ABX023-1) eluted by 80% MeOH/H_2O from the reversed-phase C18 column. HRESI(+)MS analysis of **7** revealed a sodium adduct consistent with the molecular formula $C_{49}H_{66}O_{18}$, requiring 17 double bond equivalents (DBEs). Detailed analysis of the 1D and 2D NMR (CD_3OD) data of 7 (Table S1) suggested the presence of a ring-rearranged angucycline skeleton (anthraquinone core substituted with 3-hydroxy-3-methylpentanoic acid at C-2), bearing a trisaccharide at C-7 (*C*-glycosylated) and a disaccharide at 12-OH (*O*-glycosylated), which were subsequently determined to be 7-*C*-β-D-olivosyl-4A-1B-α-L-rhodinosyl-4B-1C-α-L-rhodinose for the trisaccharide and 12-*O*-α-L-rhodinosyl-4D-1E-α-L-rhodinose for the disaccharide by independent COSY, TOCSY, HMBC, and ROESY NMR analyses. Structural assignment of 7 was further confirmed by comparison of the 1D NMR and MS spectroscopic data of 7 with those of a previously reported compound, which was considered as a shunt/acid-hydrolyzed product in the biosynthesis of grincamycin (where a C–C bond is formed between C-1 and C-14) in *Streptomyces lusitanus* SCSIO LR32.[7] Therefore, the major metabolite 7 was identified as a ring-rearranged angucyclines and was given the trivial name grincamycin O to facilitate the following structure elucidations, as this compound was previously not granted a name.

Grincamycin P (**1**) was isolated as a yellow powder. It displays the same diagnostic UV–vis maximum absorptions (λ_{max} 259, 295, and 442 nm) as those of 7 for anthraquinone-bearing compounds (Figure S3).[8] HRESI(+)MS analysis of **1** returned a sodium adduct ion attributed to the molecular formula $C_{37}H_{46}O_{14}$, requiring 15 DBEs. Analysis of the HRMS and 1D NMR (CD_3OD) data of **1** (Table 1) revealed a close similarity to those of 7, with the major differences being (i) the absence of a 2× $C_6H_{10}O_2$ subunit, (ii) the absence of two anomeric carbons ($\delta_{C\text{-}1D}$ 92.7, $\delta_{C\text{-}1E}$ 100.0), and (iii) the significantly altered chemical shifts for C-12 ($\Delta\delta_C$ −5.6) and C-15 ($\Delta\delta_C$ +3.5). These observations suggested that the di-α-L-rhodinose moieties linked to 12-OH in 7 are absent in *1*, which was further supported by the disappearance of HMBC correlation from the anomeric proton H-1D to C-12 of the 3-hydroxy-3-methylpentanoic acid side chain in **1**. The configuration of the sugar residues in **1** was established by the key NOESY correlations (Figure 2) and the comparison of 1D NMR with **7**, identifying **1** as α-L-rhodinosyl-(1 → 4)-α-L-rhodinosyl-(1 → 4)-vineomycinone B2, which was given the trivial name grincamycin P. The absolute configuration of C-12 on the side chain in **1** was assigned as *R* as evidenced from acid hydrolysis to **8** (Figure S2), comparison of specific rotations, and biosynthetic considerations (see below).

Grincamycin Q (**2**) was isolated as a yellow amorphous powder. HRESI(+)MS analysis of **2** revealed a protonated molecule attributed to the molecular formula $C_{37}H_{43}NO_{14}$, requiring 17 DBEs. Comparison of the 1D NMR (CD_3OD) data for **2** (Table 1) with **1** exhibited that the main differences lie in the replacement of two methylene groups ($\delta_{H\text{-}1B}$ 1.74/1.94, $\delta_{C\text{-}1B}$ 30.9; $\delta_{H\text{-}1C}$ 1.82, $\delta_{C\text{-}1C}$ 28.5) and one oxymethine ($\delta_{H\text{-}4C}$ 3.16, $\delta_{C\text{-}4C}$ 73.0) in **1** by an oxygenated/nitrogenated/sulfurated nonprotonated carbon ($\delta_{C\text{-}2C}$ 165.5), a sp^2 methine ($\delta_{H\text{-}3C}$ 5.14, $\delta_{C\text{-}3C}$ 94.3), and a ketone carbonyl ($\delta_{C\text{-}4C}$ 197.3) in **2**. Detailed 2D NMR analysis of **2** (Figure S2) located the modifications on the third sugar

moiety (α-L-rhodinose) of the trisaccharide in **1**, where an unusual unsaturated trideoxy keto sugar contributing to three DBEs is formed, as supported by the HMBC correlations from H-1C to C-2C and C-3C, from H-3C to C-4C and C-5C, and from H-6C to C-4C. The connection of a secondary amine to C-2C in the trideoxy keto sugar, resulting in an aminosugar rednose in **2**, was confirmed by the deshielded C-2C (δ_C 165.5) and the molecular formula $C_{37}H_{43}NO_{14}$ proposed by HRMS (Figure S5). The rare aminosugar rednose was previously reported in four anthracycline and angucycline analogues, i.e., CG21-C,[9] rudolphomycin,[10] and saquayamycins H and I.[11] These observations, together with diagnostic 2D NMR correlations (Figure 1), permitted the assignment of **2** as α-L-rednosyl-(1 → 4)-α-L-rhodinosyl-(1 → 4)-vineomycinone B2, which was subsequently named grincamycin Q, with the absolute configuration identical to **1** on the basis of NOE correlations and biosynthetic links to **1**.

Grincamycin R (**3**) was isolated as a yellow amorphous powder. HRESI(+)MS analysis of 3 revealed a sodium adduct ion indicative of a molecular formula $C_{50}H_{64}O_{18}S$, requiring 19 DBEs. Comparison of the 1D NMR (CD_3OD) data for **3** (Table 1) with those for grincamycin O (**7**) revealed the disappearance of resonances for two methylene groups ($\delta_{H\text{-}1B}$ 1.74/1.95, $\delta_{C\text{-}1B}$ 30.9; $\delta_{H\text{-}1C}$ 1.81, $\delta_{C\text{-}1C}$ 28.5) and one oxymethine ($\delta_{H\text{-}4C}$ 3.16, $\delta_{C\text{-}4C}$ 72.8) in **7**. Instead, comparable with **2**, the resonances for an oxygen/nitrogen/sulfur-substituted nonprotonated carbon ($\delta_{C\text{-}2C}$ 165.4), a sp^2 methine ($\delta_{H\text{-}3C}$ 5.14, $\delta_{C\text{-}3C}$ 116.8), and a ketone carbonyl ($\delta_{C\text{-}4C}$ 195.2) were observed in **3**, implying the oxidation of one terminal rhodinose moiety belonging to either C-7-trisaccharide or C-12-*O*-disaccharide. Diagnostic HMBC and COSY NMR correlations of **3** (Figure 1) supported this assumption and permitted determination of the modification on the terminal α-L-rhodinose moiety in C-7-trisaccharide substructure, which bears a β-heteroatom-substituted α,β-unsaturated keto group (C-2 substituted α-L-aculose). Surprisingly, compared to the *N*-substituted α,β-unsaturated keto group in **2** (Table 1), C-3C in **3** is significantly deshielded (Δ +22.5 ppm), suggesting that the β-position is substituted by a heteroatom other than nitrogen. Furthermore, the presence of resonance for an additional methyl singlet ($\delta_{H\text{-}7C}$ 2.41, $\delta_{C\text{-}7C}$ 13.9) that shows an exclusive HMBC correlation to C-2C (Figure 1), together with the comparison of 1D NMR data with those for the thiomethyl group (δ_H 2.24, δ_C 14.5) in eutypellazine A,[12] demonstrated a C-2 methylthio-substitution of the terminal α-L-aculose moiety of C-7-trisaccharide in **3**. The absolute configuration of **3** was assigned to be identical to **1** based on NOE correlations (Figure 2) and biosynthetic consideration. Thus, the structure of **3** was established as 7-[α-L-methylthio-aculosyl-(1 → 4)-α-L-rhodinosyl-(1 → 4)]-12-*O*-[α-L-rhodinosyl-(1 → 4)-α-L-rhodinosyl-(1 → 4)]-vineomycinone B2, which was named grincamycin R. This is the first time to report a 2-methylthio-α-L-aculose moiety that has been found in nature, and **3** is the founding member that possesses this novel sugar moiety.

Grincamycin S (**4**) was isolated as a red amorphous powder, whose UV–vis spectrum shows obvious red-shifted absorptions (229 → 234 nm, 441 → 496 nm) compared to those for **1–3** (Figure S3). This suggests the presence of a larger conjugated system in **4.** HRESI(+)MS analysis of **4** revealed a molecular formula $C_{37}H_{46}O_{15}$, suggestive of a hydroxylated analogue of **1** with 15 DBEs. Comparison of 1D NMR (CD_3OD) data for **4** (Table 1) with

1 supported this hypothesis, with the only significant difference being C-4 hydroxylation of the anthraquinone backbone evident from (i) the disappearance of one doublet aromatic proton ($\delta_{H\text{-}4}$ 7.81, $\delta_{C\text{-}4}$ 119.6); (ii) the presence of an additional oxygen-bearing aromatic nonprotonated carbon ($\delta_{C\text{-}4}$ 158.2); (iii) the replacement of a doublet aromatic proton ($\delta_{H\text{-}3}$ 7.77, $\delta_{C\text{-}3}$ 140.8) with a singlet ($\delta_{H\text{-}3}$ 7.38, $\delta_{C\text{-}3}$ 132.5); and (iv) the significantly altered chemical shifts for C-1 ($\Delta\delta_C$ −3.6), C-2 ($\Delta\delta_C$ +6.4), C-3 ($\Delta\delta_C$ −8.3), and C-4a ($\Delta\boldsymbol{\delta}_C$ −20.5). The HMBC correlation from H-3 to C-4 further validated this conclusion (Figure 1). Thus, **4** was determined as 4-hydroxygrincamycin P, which was subsequently given the trivial name grincamycin S.

Grincamycin T (**5**) was isolated as a red amorphous powder. It displays the same UV–vis absorption as that of **4**, implying the possession of a 4-hydroxy-anthraquinone aglycone in **5**. HRESI(+)MS analysis of **5** returned a molecular formula $C_{49}H_{66}O_{19}$ requiring 17 DBEs. Compared to **4**, the increase in molecular weight (228 Da) of **5** exactly matches those for two rhodinose residues (2× $C_6H_{10}O_2$), suggestive of an additional disaccharide substitution. Comparison of 1D NMR (CD_3OD) data for **5** (Table 1) with those for grincamycin O (**7**) revealed the absence of resonance for an aromatic proton ($\delta_{H\text{-}4}$ 7.54, $\delta_{C\text{-}4}$ 119.4) and the appearance of resonances for an oxygen-bearing nonprotonated carbon ($\delta_{C\text{-}4}$ 158.1), as well as decoupling of the aromatic proton attached to C-3 ($\delta_{H\text{-}3}$ 7.47, singlet). Moreover, we observed remarkable changes in chemical shifts for C-1 ($\Delta\delta_C$ −3.2), C-2 ($\Delta\delta_C$ +6.9), C-3 ($\Delta\delta_C$ −8.1), C-4a ($\Delta\delta_C$ −20.2), and C-5 ($\Delta\delta_C$ +3.3) in **5** compared to those in **7**, which are very similar to **4**. Based on the above observations, together with the diagnostic HMBC correlation from H-3 to C-4 (Figure 1), **5** was assigned to be C-4 hydroxylated derivative of grincamycin O, which was named as grincamycin T.

Apart from the major metabolite grincamycin O (**7**) and the new metabolites grincamycins P–T (**1**–**5**), other known metabolites in the same structure class, i.e., grincamycin L (**6**),[13] vineomycinone B2 (also known as fridamycin A) (**8**),[14] and vineomycin E (**9**),[14] were also isolated from the PMP-active fractions and structurally identified on the basis of detailed spectroscopic analysis (Table S1). Particularly, **8** is a rearranged angucycline with only one deoxy sugar (i.e., β-D-olivose) in the structure, whose 1D NMR data and specific rotation are almost consistent with those for vineomycinone B2 methyl ester.[15] Thus, the absolute configuration of C-12 in the 3-hydroxy-3-methylpentanoic acid side chain is tentatively assigned as *R*, which is identical to vineomycinone B2 and other rearranged angucyclines reported so far.[13,14,16,17] It is also worth mentioning that **9** possesses an unusual deoxy sugar 4-dihydro-L-cinerulose B and forms 1 → 4 glycosidic bond and 2 → 3 ether bond with β-D-olivose, which has only been reported in **9** and the other *Streptomyces* metabolite, PI-083, to date.[18]

In the course of compound purification, we noticed that the *O*-glycosidic bonds of the rearranged angucyclines were inclined to hydrolyze under acidic conditions (0.1% formic acid or TFA). To evaluate acid stability of the purified glycosides, selected compounds (i.e., **1**, **2**, **4**, **5**, **8**, **9**) were incubated in 0.1% TFA/MeOH solution at 30 °C for 12 h. LC-MS results revealed that **1**, **2**, **4**, and **5** were almost fully converted into **8** (Figure S2), which only retains an acid-resistant *C*-glycosidic bond. This suggests that the *O*-glycosidic bonds in angucyclines are acid labile. In contrast, **9** showed resistance to 0.1% TFA probably due

to the formation of an additional 1 → 4 *O*-glycosidic bond and a 2 → 3 ether bond (Figure S2). In addition, the acid hydrolysis result further confirmed that **1–5** bear the same aglycon as that of vineomycinone B2 (**8**), including the absolute configuration.

Grincamycins are a large group of compounds belonging to the class of angucycline glycosides produced by actinomycetes. The founding member grincamycin (grincamycin A), discovered from *Streptomyces griseoincarnatus* in 1987,[19] possesses a tetrangomycin-like aglycon (aglycon I). However, the other grincamycin members have varied aglycon structures (Figure 3). For example, grincamycins B—D, L, and K feature a rearranged tricyclic aglycon (aglycon II) instead of the tetracyclic core structure in grincamycins A, I, J, and M,[13,14,16,17,20] while grincamycins E, G, H, and N have a linear tetracyclic anthraquinone aglycone (aglycon III).[16,17] Interestingly, other trivial names have been applied to angucyclines bearing the same aglycons by different research groups, such as vineomycins for aglycons I and II-containing angucyclines,[14,17] and saquayamycins for aglycon I only,[11] where the major structural differences lie in the varied deoxy sugar moieties attached to the aglycons. It was previously observed that aglycon I can be converted into aglycon II under acidic condition and converted to aglycon III by UV irradiation (Figure 3).[7] Given that all of the grincamycins isolated from *Streptomyces* sp. CNZ-748 in the present study possess the tricyclic aglycon II, which might be generated during solvent extraction and isolation, we recultivated the strain in the same media used for compounds isolation and carefully performed EtOAc extraction avoiding acid and light. However, an array of the same rearranged angucycline glycosides bearing aglycon II remained the predominant metabolites in the extract. To investigate the impact of culture media on aglycon production, we grew *Streptomyces* sp. CNZ-748 in the modified RA medium (previously used for the production of grincamycins bearing aglycons I, II, and III by *Streptomyces lusitanus* SCSIO LR32) and SG medium (previously used for saquayamycin production by *Streptomyces* sp. KY40-1), respectively.[11,16] Although the culture media and conditions were strictly followed as described in the literature, aglycon II-containing grincamycins remained the major angucyclines in the extract of *Streptomyces* sp. CNZ-748 cultured in SG medium. To our surprise, the production of grincamycins is almost abolished when the strain was cultivated in the modified RA medium. Taken together, these results suggest that the production of aglycon II-containing grincamycins in *Streptomyces* sp. CNZ-748 may be genetically encoded and regulated by the corresponding biosynthetic genes.

To further explore possible underlying reasons for the various forms of the angucycline aglycons, we sequenced the genome of the producing strain *Streptomyces* sp. CNZ-748. The assembled genome was 7.62 Mbp with 72% GC and consisted of 182 contigs (N50 = 69 524 bp). Genome annotation was performed with PROKKA and run through antiSMASH v5.0,[21] resulting in the detection of 19 BGCs (Figure 4B). A previous study reported that the biosynthesis of grincamycins (derived from deep-sea sediments) in *Streptomyces lusitanus* strain SCSIO LR32 is encoded by a bacterial type II polyketide synthase (T2PKS) BGC that includes multiple glycosyltransferases, dehydratases, and many other potential accessory enzymes.[7] Using these biosynthetic enzymes as queries, we identified a 66 kbp T2PKS hybrid BGC that likely accounts for the biosynthesis of grincamycins in *Streptomyces*

sp. CNZ-748 (Figure 4C; Table S2). Next, we compared the predicted grincamycin BGC (*gcn*-CNZ748) in *Streptomyces* sp. CNZ-748 with the corresponding BGC (*gcn*-LR32) found in *Streptomyces lusitanus* SCSIO LR32[7] and the saquayamycin BGC (*sqn*) from *Streptomyces* sp. KY40-1.[22] Using clinker and clustermap,[23] we visualized homologous genes shared between these BGCs (Figure 4D) and observed high synteny for the key polyketide synthases (involved in the formation of the angucycline aglycon) and the glycosyltransferases and dehydratases (responsible for the installation and modification of the saccharide moieties). However, these BGCs varied in their auxiliary gene content located upstream and downstream of the core biosynthetic genes (Figure 4D). For example, the downstream genes (far-right) *gcnT* and *gcnU,* encoding two putative oxidoreductases in *gcn*-LR32 and *sqn,* are absent in *gcn*-CNZ748. In contrast, the upstream genes (far-left) *orf2* (coding for nucleotidyltransferase family protein), *orf3* (malate synthase A), *orf5* (hypothetical protein), and *orf6* (oxidoreductase, GcnA) are present in both *gcn*-CNZ748 and *gcn*-LR32 but are missing in *sqn.* In addition, *orf4* (SelT/SelW/SelH family protein) is exclusively present in *gcn*-CNZ748. Finally, the presence of a monooxygenase FAD-binding protein is ambiguous in the *gcn*-CNZ748 BGC due to a conflicting annotation with a tRNA-Ala(ggc). At present, we cannot determine if these differences in auxiliary genes are related to the generation of different aglycons, as their functions remain to be experimentally validated. Thus, a detailed genetic and biochemical investigation regarding the formation of different types of aglycons in grincamycins will follow in a separate study.

Interestingly, the *gcn* BGC was not observed in any of the 16 strains with genome sequences that are most closely related to CNZ-748 (Figure 4A). This includes two strains, *Streptomyces tendae* 139 and *Streptomyces* sp. CNH-189, which belong to the same species based on sharing >95% average nucleotide identity (ANI) (Figure S64). The *gcn* BGC is the only “singleton” observed in the CNZ-748 genome, suggesting it may have been acquired by horizontal gene transfer.

Angucyclines have been reported to possess promising antitumor activities even against multidrug-resistant cancer cells.[24] Thus, this class of compounds is considered as a potential source for anticancer drug discovery, as exemplified by landomycin A, the most potent anthracycline related anticancer angucycline antibiotic.[25] As an expanding class of angucycline glycosides, the rearranged grincamycins also displayed comparable inhibitory activities against various cancer cell lines.[14,16,17] In order to discover potential small molecule leads combating the rare cancer PMP, we evaluated the cytotoxic effect of grincamycins **1**–**9** on three PMP cell lines (PMP501-1, PMP457-2, and ABX023-1) and one related cell line (C09-1) from a peritoneal metastasis of a colonic mucinous adenocarcinoma, which we recently isolated and passaged *in vitro.* The crystal violet assay (Table 2, Figure S65) revealed that several compounds tested inhibited the proliferation of various cell lines tested, showing IC_{50} values ranging from 2.5 to 61 μM. Particularly, **4** and **5**, which bear 4-hydroxy on the anthraquinone aglycon, are the most active against all cell lines, suggesting that hydroxylation of C-4 can enhance the cytotoxic potency of grincamycins. Furthermore, **3** possesses a unique sulfur-containing α-L-methylthio-aculose terminal sugar residue and displayed cytotoxicity toward PMP501-1 and PMP457-2. The compound possessed a 1.5–5 fold increased potency over **7**, which contains the common

deoxy sugar α-L-rhodinose at the end of the saccharide chain. These observations on the improved potency of **3–5** imply that the substitution of the angucycline aglycon with a 4-hydroxy group or the terminal sugar of the trisaccharide with a methylthio group can increase cytotoxicity toward PMP cell lines. These structural changes may help improve the solubility of angucyclines and facilitate a stronger interaction between the compounds and their target.

In conclusion, this report documents the bioassay-guided fractionation of compounds from the marine-derived *Streptomyces* sp. CNZ-748, leading to the discovery of five new rearranged angucyclines grincamycins P—T (**1–5**), together with four known grincamycins **6–9**, which exhibited inhibitory activities toward PMP cells. The chemical structures of the isolated grincamycins were unambiguously established based on spectroscopic and chemical analyses. Particularly, **3** possesses an *S*-containing α-L-methylthio-aculose residue, which was reported in nature for the first time, while **2** bears a rare *N*-containing α-L-rednose sugar moiety. Genome sequencing of the producer *Streptomyces* sp. CNZ-748 and comparative BGC analysis led us to propose the BGC of gricamycins isolated in this study and to further propose the mechanism for the production of the rearranged angucycline aglycon. Cell viability assay demonstrated that the thio deoxy sugar-bearing grincamycin (i.e., **3**) and the C-4 hydroxylated grincamycins (i.e., **4** and **5**) have increased cytotoxic activities toward most of the PMP cell lines tested. Our study expands the chemical diversity of rearranged angucycline glycosides and inspires the design and development of small molecule therapies for combating the rare cancer pseudomyxoma peritonei (PMP).

EXPERIMENTAL SECTION

General Experimental Procedures.

Optical rotations were measured on a JASCO P-1010 polarimeter in a 100 mm × 2 mm cell at room temperature. UV–vis spectra were obtained on a Jasco V-730 UV–vis spectrophotometer with 1 cm quartz cells. Infrared (IR) spectra were acquired on a PerkinElmer Spectrum 100 FT-IR spectrometer. Nuclear magnetic resonance (NMR) spectra were acquired on either a Bruker Avance III HD 400 MHz spectrometer with a 5 mm BBO 1*H*/19F-BB-Z-Gradient prodigy cryoprobe, a Bruker Avance III HD 500 MHz spectrometer with a PA BBO 500S2 BBF-H-D_05 Z SP probe, or a Bruker Avance III HD Ascend 700 MHz equipped with 5 mm triple-resonance Observe (TXO) cryoprobe with Z-gradients, controlled by TopSpin 3.6.1 software. In all cases, spectra were acquired at 25 °C (unless otherwise specified) in solvents as specified in the text, with referencing to residual ^{1}H or ^{13}C signals in the deuterated solvent (δ_H 3.31 and δ_C 49.0 for CD_3OD). High-resolution ESIMS spectra were obtained on a Thermo Scientific Orbitrap Velos Pro hybrid ion trap-orbitrap mass spectrometer by direct injection. Liquid chromatography–diode array–electrospray ionization mass spectrometry (LC-DAD-ESIMS) data were acquired on a Thermo Dionex Ultimate 3000 UHPLC system equipped with a diode array multiple wavelength detector and an LTQ XL linear ion trap mass spectrometer controlled by Thermo Xcalibur (version 4.2.47). The sheath gas was at a flow rate of 35 arbitrary units, and the source heater temperature of 325 °C and capillary temperature of 350 °C were set for the ion trap mass spectrometer. Semipreparative HPLC purifications were performed using

the Thermo Dionex Ultimate 3000 HPLC system with corresponding pump, autosampler, UV–vis detectors, fraction collectors, and Chromeleon software (version 7.2.10), inclusively. LCMS-grade and HPLC-grade CH_3CN, H_2O, and formic acid were purchased from Fisher Scientific. Deuterated solvents were purchased from Cambridge Isotopes.

Strain Isolation.

The strain *Streptomyces* sp. CNZ-748 was isolated from a marine sediment sample collected at South San Diego Bay, California, USA, in July 2018. The sediment was dried for 72 h in a laminar flow hood and stamped using an autoclaved foam plug onto sterile agar plates of the medium SWA (1.6%, seawater) modified from Jensen et al. (2005).[26] A colony of CNZ-748 was picked from the isolation plate and passaged onto A1 agar (1% soluble starch, 0.4% yeast extract, 0.2% peptone, 2.8% Instant Ocean Aquarium Sea Salt, 1.6% agar) until a pure colony was formed.

Genome Sequencing, Assembly, and BGC Analysis.

Strain CNZ-748 was inoculated from a frozen stock into a 125 mL Erlenmeyer flask containing 50 mL of A1 broth and shaken at 220 rpm, 25 °C, for 4 days. Genomic DNA was extracted using 1.5 mL of cell suspension and purified using the Wizard Genomic DNA Purification kit (Promega) with amendments for Gram-positive bacteria. Briefly, cellular lysis was aided by incubation with 60 μL of lysozyme for 45 min at 37 °C. Genome sequencing and library preparation was carried out at the Microbial Genome Sequencing Center (MiGS) using Illumina NextSeq 550 technology. Raw reads were quality trimmed and adapters removed using BBMap (trimq = 10, qtrim = rl). Quality filtered reads were assembled using the SPAdes genome assembler with a “careful” iterative *k*-step ranging from $k = 31$ to 111.[27] The resulting assembly was assessed using a taxon-annotated-GC-coverage (TAGC) plot, which calculates contig coverage and taxonomic hits to the NCBI database. Based on the results from the TAGC-plots, we discarded all contigs with coverage < 30*x*, length < 2000 bp, and GC% < 55%. Genome annotation was performed using PROKKA with the resulting annotated genome analyzed by antiSMASH v5.0 for BGC prediction.[21]

The closest reference genome to strain CNZ-748 was identified as *Streptomyces tendae* (95.9% average nucleotide identity; Figure S64) using the Microbial Genomes Atlas (MiGA).[28] Closely related genomes collated from the Genome Taxonomy Database[29] ($N = 16$) were used to create a multilocus phylogeny with 21 single-copy phylogenetic marker genes.[30] Each marker gene was independently aligned using ClustalO v1.2.4[31] and concatenated to create a protein alignment (3544 amino acids) for phylogenetic analysis using RAxML v8.2.12[32] under the PROTGAMMABLOSUM model for 100 replicates. BGCs from CNZ-748 and related genomes (analyzed as per CNZ-748) were clustered into gene cluster families (GCFs) with BiG-SCAPE to assess the distribution of the *gcn* BGC. The comparative BGC analysis of *gcn*-CNZ-748, *gcn*-LR32, and *sqn* was performed using the clinker and clustermap.js program, which enables automatic visualization of gene cluster comparisons.[23]

Cultivation, Extraction, and Fractionation of *Streptomyces* sp. CNZ-748.

A loop of spores of *Streptomyces* sp. CNZ-748 was inoculated in a 50 mL conical tube containing 15 mL of A1 broth and shaken at 220 rpm, 30 °C, for 5 days. The first batch of seed culture (15 mL) was transferred into a 2.5 L Ultra Yield flask (Thomson Scientific) containing 500 mL of A1 broth and cultivated under the same condition for 2 days. The resulting second batch of seed culture was used to inoculate 2.5 L Ultra Yield flasks (20×) with each containing 600 mL of A1 broth, which were subsequently shaken at 220 rpm at 30 °C for 9 days. The bacterial broth was extracted with an equal volume of EtOAc, and the combined organic phase was concentrated *in vacuo* to yield the extract (1.6 g), which was partitioned on a reversed-phase C_{18} open column with a 10% stepwise gradient elution from 90% H_2O/MeOH to MeOH.

The 20% H_2O/MeOH fraction (315.8 mg) was loaded onto Sephadex LH-20 column eluting with MeOH to afford 30 subfractions (Frs. 1–30). Fr. 3 (4.5 mg) was further purified by HPLC (Phenomenex Luna RP-C_{18}, 250 mm × 10 mm, 5 μm, 100 Å, 3.5 mL/min isocratic elution at 34% H_2O/MeCN over 30 min with constant 0.1% formic acid) to yield grincamycin R (**3**) (t_R = 20.0 min, 0.6 mg). The combined Frs. 4–7 (146.9 mg) were further fractionated by HPLC (Phenomenex Luna RP-C_{18}, 250 mm × 10 mm, 5 μm, 100 Å, 3.5 mL/min isocratic elution at 50% H_2O/MeCN over 30 min) to generate grincamycin S (**4**) (t_R = 13.4 min, 0.7 mg), grincamycin O (**7**) (t_R = 23.4 min, 13.9 mg), and grincamycin T (**5**) (t_R = 25.9 min, 1.3 mg). The combined Frs. 10–13 (82.9 mg) were fractionated by HPLC (Waters XBridge Prep C_{18} OBD column, 150 mm × 19 mm, 5 μm, 100 Å, 7.0 mL/min gradient elution from 55 to 10% H_2O/MeCN over 20 min) to give grincamycin L (**6**) (t_R = 7.8 min, 6.5 mg), vineomycin E (**9**) (t_R = 8.2 min, 1.8 mg), and grincamycin Q (**2**) (t_R = 8.9 min, 1.4 mg).

The 30% H_2O/MeOH fraction (197.5 mg) was subjected to Sephadex LH-20 chromatography eluting with MeOH to give 35 subfractions. The combined Frs. 8–11 (34.8 mg) were fractionated by HPLC (Phenomenex Luna RP-C_{18}, 250 mm × 10 mm, 5 μm, 100 Å, 3.5 mL/min gradient elution from 60 to 20% H_2O/MeCN over 40 min with constant 0.1% formic acid) to give grincamycin P (**1**) (t_R = 23.6 min, 4.0 mg). The Frs. 13–16 (20.4 mg) were combined and resolved by HPLC (Waters XBridge BEH C_{18} OBD Prep column, 150 mm × 10 mm, 5 μm, 130 Å, 3.5 mL/min isocratic elution at 70% H_2O/MeCN over 30 min with constant 0.1% formic acid) to yield vineomycinone B2 (**8**) (t_R = 13.7 min, 8.2 mg).

Grincamycin P (1).—This compound is a yellow amorphous powder; $[\alpha_D^{23}$ −11 (c 0.1, MeOH); UV–vis (MeOH) λ_{max} (log ε) 259 (4.38), 295 (3.97), 442 (4.01) nm; IR νmax 3391, 2945, 2935, 2877, 1722, 1625, 1582, 1421, 1374, 1251, 1117, 1049, 995 cm^{-1}; NMR (500 MHz, CD_3OD), Table 1; HRMS (ESI-Orbitrap) m/z 737.2783 $[M + Na]^+$ (calcd for $C_{37}H_{46}O_{14}Na^+$, 737.2780).

Grincamycin Q (2).—This compound is a yellow amorphous powder; $[\alpha]_D^{23}$ +230 (c 0.15, MeOH); UV–vis (MeOH) λ_{max} (log ε) 259 (4.37), 294 (4.28), 440 (3.93) nm; NMR (500 MHz, CD_3OD), Table 1; HRMS (ESI-Orbitrap) m/z 726.2754 $[M + H]^+$ (calcd for $C_{37}H_{44}NO_{14}^+$, 726.2756).

Grincamycin R (3).—This compound is a yellow amorphous powder; $[\alpha]_D^{23}$ −85 (*c* 0.04, MeOH); UV–vis (MeOH) λ_{max} (log ε) 259 (4.24), 294 (4.15), 441 (3.90) nm; NMR (700 MHz, CD_3OD), Table 1; HRMS (ESI-Orbitrap) *m/z* 1007.3706 $[M + Na]^+$ (calcd for $C_{50}H_{64}O_{18}SNa^+$ 1007.3714).

Grincamycin S (4).—This compound is a red amorphous powder; $[\alpha]_D^{23}$ −400 (*c* 0.05, MeOH); UV–vis (MeOH) λ_{max} (log ε) 255 (4.20), 295 (3.65), 497 (3.88) nm; NMR (700 MHz, CD_3OD), Table 1; HRMS (ESI-Orbitrap) *m/z* 753.2727 $[M + Na]^+$ (calcd for $C_{37}H_{46}O_{15}Na^+$, 753.2729).

Grincamycin T (5).—This compound is a red amorphous powder; $[\alpha]_D^{23}$ −220 (*c* 0.12, MeOH); UV–vis (MeOH) λ_{max} (log ε) 255 (4.26), 296 (3.72), 497 (3.97) nm; NMR (700 MHz, CD_3OD), Table 1; HRMS (ESI-Orbitrap) *m/z* 981.4086 $[M + Na]^+$ (calcd for $C_{49}H_{66}O_{19}Na^+$, 981.4092).

Acid-Mediated Degradation of Grincamycins.

Aliquots (10 μg) of the selected compounds (**1, 2, 4, 5, 8,** and **9**) were treated with 0.1% TFA in MeOH (50 μL) at 30 °C for 12 h, respectively, after which the reaction mixtures were concentrated to dryness under N_2. The samples were redissolved in MeOH (30 μL) and analyzed on UHPLC-DAD-ESI(±)MS (Kinetex XB-C_{18} column, 100 mm × 2.1 mm, 2.6 μm, 0.5 mL/min gradient elution from 90% H_2O/MeCN to 100% MeCN over 10 min, with constant 0.1% formic acid modifier). Authentic standards of each compound were analyzed by the same LC-MS method.

Cytotoxicity Assay of Compounds 1–9 against PMP Cell Lines.

The cytotoxicities of **1–9** against three PMP cell lines (PMP501-1, PMP457-2, and ABX023-1) and one cell line from a peritoneal metastasis of a colonic mucinous adenocarcinoma (C09-1) were measured using crystal violet assay. PMP501-1 and PMP457-2 originated from well-differentiated tumors. C09-1 represents peritoneal metastasis of a moderately differentiated mucinous colonic adenocarcinoma. The PMP cells (200 μL) were plated in 96-well microtiter plates in triplicate at a density of 30 000 cells per well in Ham's F12 growth medium supplemented with 10% fetal bovine serum, 146 mg/L L-glutamine, 10 μg/mL insulin, and 5 ng/mL sodium selenite. The cells were allowed to incubate at 37 °C for 24 h and then treated with the tested compounds followed by incubation for another 24 h. Each set of treatments also contained a DMSO vehicle control, a positive control (5-fluorouracil), and a dead-cell control (by treating cells with a solution of 10% EtOH in growth medium). After the 24 h treatment period, cells were washed with PBS and then stained with a 0.2% crystal violet solution. After incubation at room temperature for 10 min, cells were washed several times with distilled H_2O to remove excess crystal violet. Subsequently, the cells were incubated in a 0.5% SDS + 50% EtOH solution on an orbital shaker for 10 min to dissolve all crystal violet in the cells. The optical density (O.D.) value of each well was measured using a spectrophotometer at a wavelength of 595 nm. The experiments were carried out in three biological replicates. Final values for each compound were taken as a percent of the average control minus the average dead-cell control in order to create dose–response curves using GraphPad Prism 9.

Supplementary Material

Refer to Web version on PubMed Central for supplementary material.

ACKNOWLEDGMENTS

This work is partially funded by National Institutes of Health (NIH) grants P20GM103641 and R01GM085770 and a National Science Foundation EPSCoR Program OIA-1655740. T.L.T. received support from the National Organization for Rare Disorders (NORD). X.T. acknowledges a partial support from Shenzhen Bay Laboratory Startup Funds (21230051). We thank Dr. P. J. Pellechia and Miss T. Johnson from UofSC NMR Facility for help with acquiring NMR data, as well as Dr. M. D. Walla and Dr. W. E. Cotham from UofSC Mass Spectrometry Facility for acquiring HRMS data (NSF-MRI program award No. 1828059). The study also made use of the Campus Chemical Instrument Center NMR facility at the Ohio State University. We also thank Mr. C. L. M. Gilchrist from The University of Western Australia for the assistance with the use of the clinker & clustermap program.

REFERENCES

(1). Fenical W; Jensen PR Nat. Chem. Biol 2006, 2, 666. [PubMed: 17108984]

(2). Newman DJ; Cragg GM J. Nat. Prod 2004, 67, 1216. [PubMed: 15332835]

(3). Molinski TF; Dalisay DS; Lievens SL; Saludes JP Nat. Rev. Drug Discovery 2009, 8, 69. [PubMed: 19096380]

(4). Gleeson EM; Feldman R; Mapow BL; Mackovick LT; Ward KM; Morano WF; Rubin RR; Bowne WB Am. J. Clin. Oncol 2018, 41, 777. [PubMed: 28263231]

(5). Carr NJ; Cecil TD; Mohamed F; Sobin LH; Sugarbaker PH; González-Moreno S; Taflampas P; Chapman S; Moran BJ Am. J. Surg. Pathol 2016, 40, 14. [PubMed: 26492181]

(6). Shaib WL; Assi R; Shamseddine A; Alese OB; Staley C; Memis B; Adsay V; Bekaii-Saab T; El-Rayes BF Oncologist 2017, 22, 1107. [PubMed: 28663356]

(7). Zhang Y; Huang H; Chen Q; Luo M; Sun A; Song Y; Ma J; Ju J Org. Lett 2013, 15, 3254. [PubMed: 23782455]

(8). MacHatova Z; Barbieriková Z; Poliak P; Jančovičová V; Lukeš V; Brezová V Dyes Pigm. 2016, 132, 79.

(9). Johdo O; Yoshioka T; Naganawa H; Takeuchi T; Yoshimoto A J. Antibiot. 1996, 49, 669.

(10). Nettleton DE; Balitz DM; Doyle TW; Bradner WT; Johnson DL; O'Herron FA; Schreiber RH; Coon AB; Moseley JE; Myllymaki RW J. Nat. Prod 1980, 43, 242. [PubMed: 7381507]

(11). Shaaban KA; Ahmed TA; Leggas M; Rohr J J. Nat. Prod 2012, 75, 1383. [PubMed: 22758660]

(12). Niu S; Liu D; Shao Z; Proksch P; Lin W RSC Adv. 2017, 7, 33580.

(13). Yang L; Hou L; Li H; Li W Nat. Prod. Res 2020, 34, 3444. [PubMed: 30835571]

(14). Qu XY; Ren JW; Peng AH; Lin SQ; Lu DD; Du QQ ; Liu L; Li X; Li EW; Xie WD Mar. Drugs 2019, 17, 277.

(15). Danishefsky SJ; Uang BJ; Quallich G J. Am. Chem. Soc 1985, 107, 1285.

(16). Huang H; Yang T; Ren X; Liu J; Song Y; Sun A; Ma J; Wang B; Zhang Y; Huang C; Zhang C; Ju J J. Nat. Prod 2012, 75, 202. [PubMed: 22304344]

(17). Zhu X; Duan Y; Cui Z; Wang Z; Li Z; Zhang Y; Ju J; Huang H J. Antibiot. 2017, 70, 819.

(18). Kawashima A; Yoshimura Y; Gotō J; Nakaike S; Mizutani T; Hanada K; Omura S J. Antibiot. 1988, 41, 1913.

(19). Hayakawa Y; Iwakiri T; Imamura K; Seto H; Ōtake N J. Antibiot. 1987, 40, 1785.

(20). Bao J; He F; Li Y; Fang L; Wang K; Song J; Zhou J; Li Q; Zhang H J. Antibiot. 2018, 71, 1018.

(21). Blin K; Shaw S; Steinke K; Villebro R; Ziemert N; Lee SY; Medema MH; Weber T Nucleic Acids Res. 2019, 47, W81. [PubMed: 31032519]

(22). Salem SM; Weidenbach S; Rohr J ACS Chem. Biol 2017, 12, 2529. [PubMed: 28892347]

(23). Gilchrist CLM; Chooi YH Bioinformatics 2021, 1.

(24). Kharel MK; Pahari P; Shepherd MD; Tibrewal N; Nybo SE; Shaaban KA; Rohr J Nat. Prod. Rep 2012, 29, 264. [PubMed: 22186970]

(25). Yang X; Fu B; Yu B J. Am. Chem. Soc 2011, 133, 12433. [PubMed: 21780843]

(26). Jensen PR; Gontang E; Mafnas C; Mincer TJ; Fenical W Environ. Microbiol 2005, 7, 1039. [PubMed: 15946301]

(27). Bankevich A; Nurk S; Antipov D; Gurevich AA; Dvorkin M; Kulikov AS; Lesin VM; Nikolenko SI; Pham S; Prjibelski AD; Pyshkin AV; Sirotkin AV; Vyahhi N; Tesler G; Alekseyev MA; Pevzner PA J. Comput. Biol 2012, 19, 455. [PubMed: 22506599]

(28). Rodriguez-R LM; Gunturu S; Harvey WT; Rosselló-Mora R; Tiedje JM; Cole JR; Konstantinidis KT Nucleic Acids Res. 2018, 46, W282. [PubMed: 29905870]

(29). Chaumeil PA; Mussig AJ; Hugenholtz P; Parks DH Bioinformatics 2019, 36, 1925.

(30). Wu D; Jospin G; Eisen JA PLoS One 2013, 8, No. e77033. [PubMed: 24146954]

(31). Sievers F; Wilm A; Dineen D; Gibson TJ; Karplus K; Li W; Lopez R; McWilliam H; Remmert M; Söding J; Thompson JD; Higgins DG Mol. Syst. Biol 2011, 7, 539. [PubMed: 21988835]

(32). Stamatakis A Bioinformatics 2014, 30, 1312. [PubMed: 24451623]

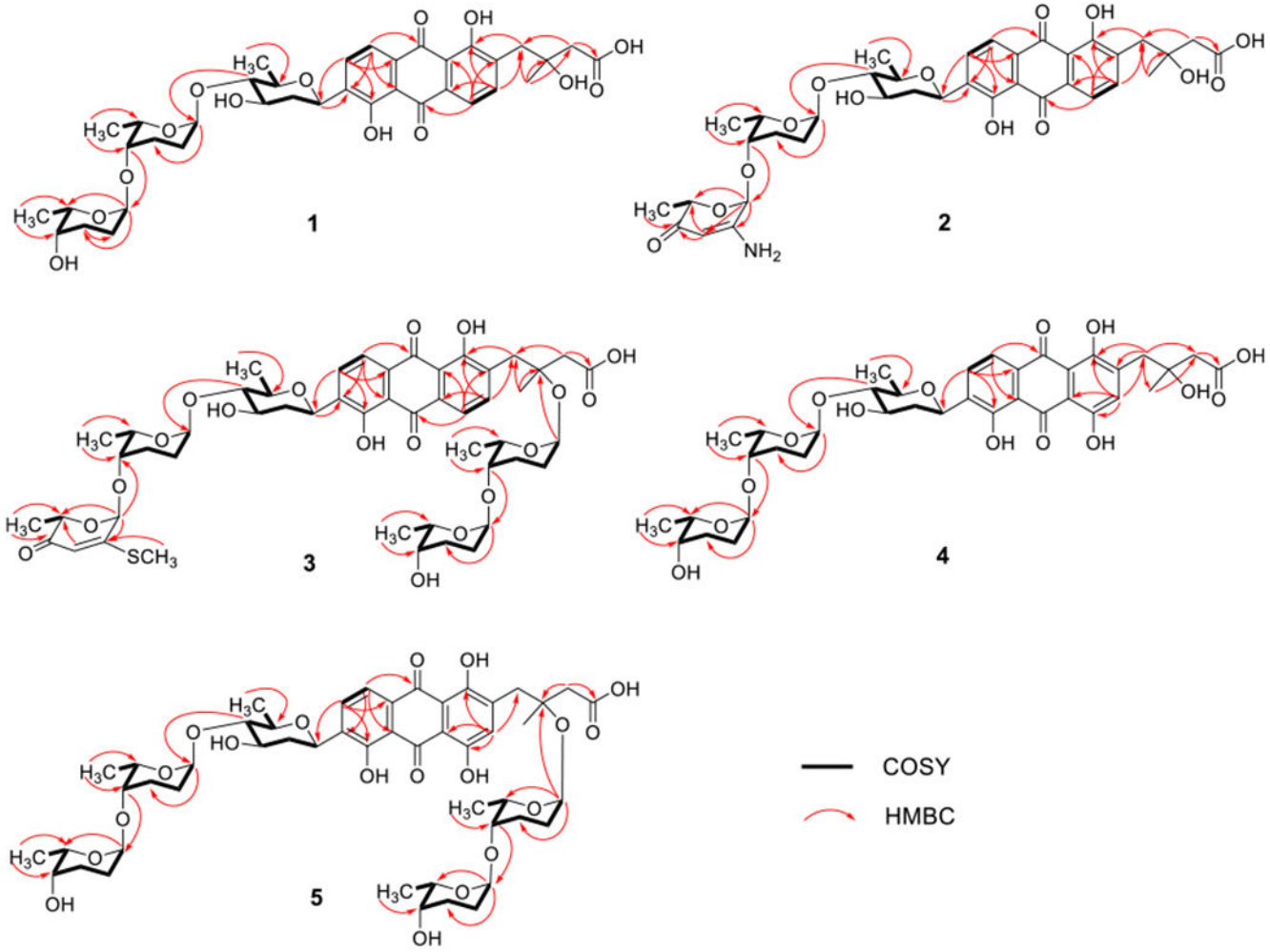

Figure 1.
Key 2D NMR (CD_3OD) correlations for **1–5**.

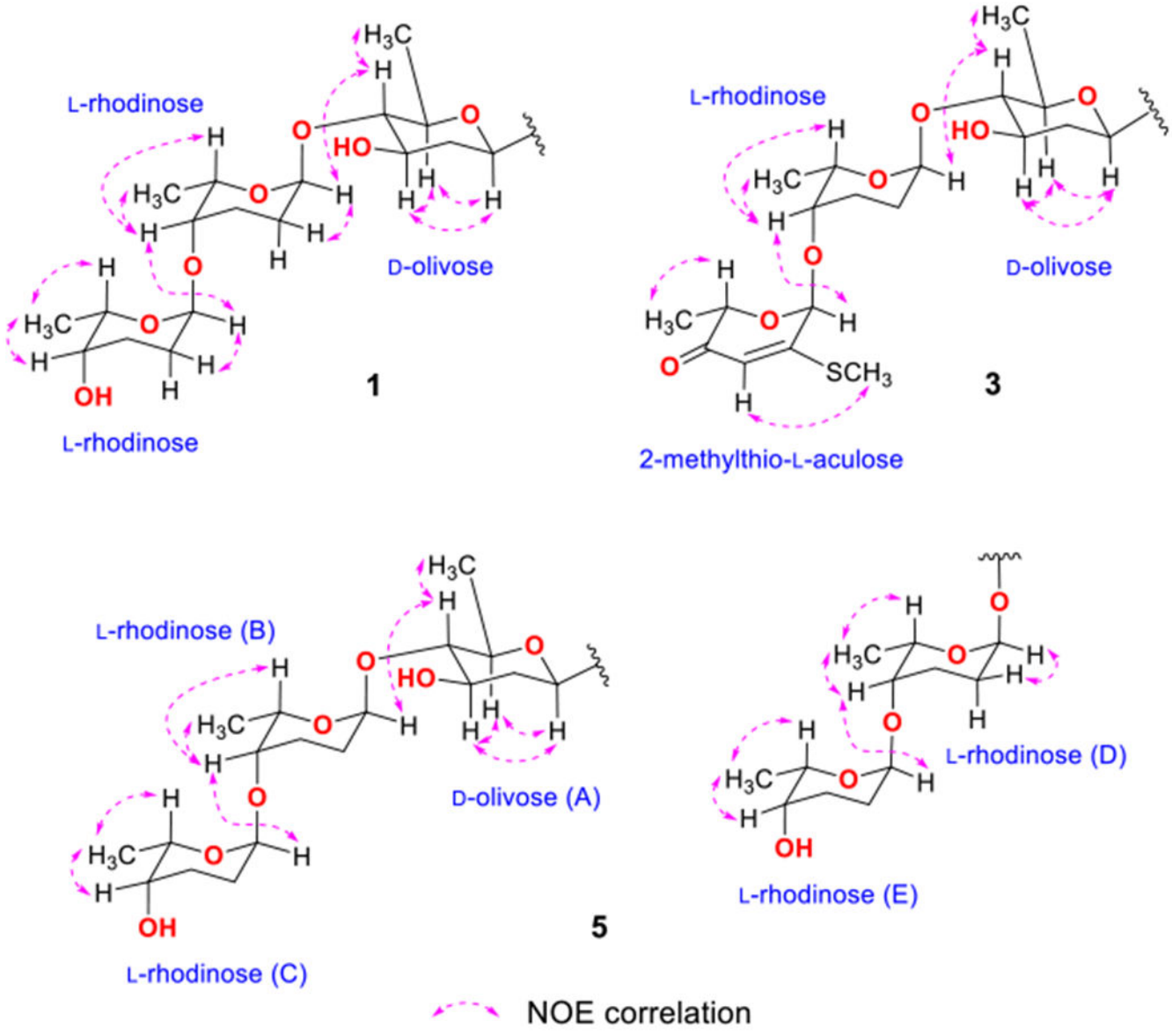

Figure 2.
Diagnostic NOE (CD_3OD) correlations for **1, 3,** and **5.**

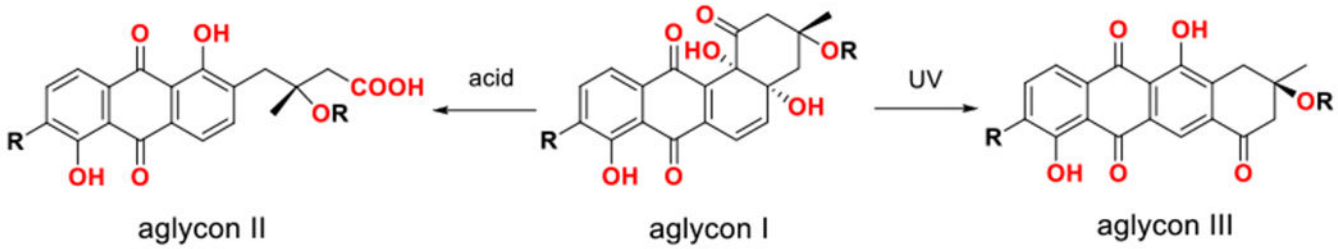

Figure 3.

Structures of angucycline aglycon (I) and its rearranged forms (II and III). It was previously proposed that the rearranged forms (II and III) may be generated under nonenzymatic conditions.

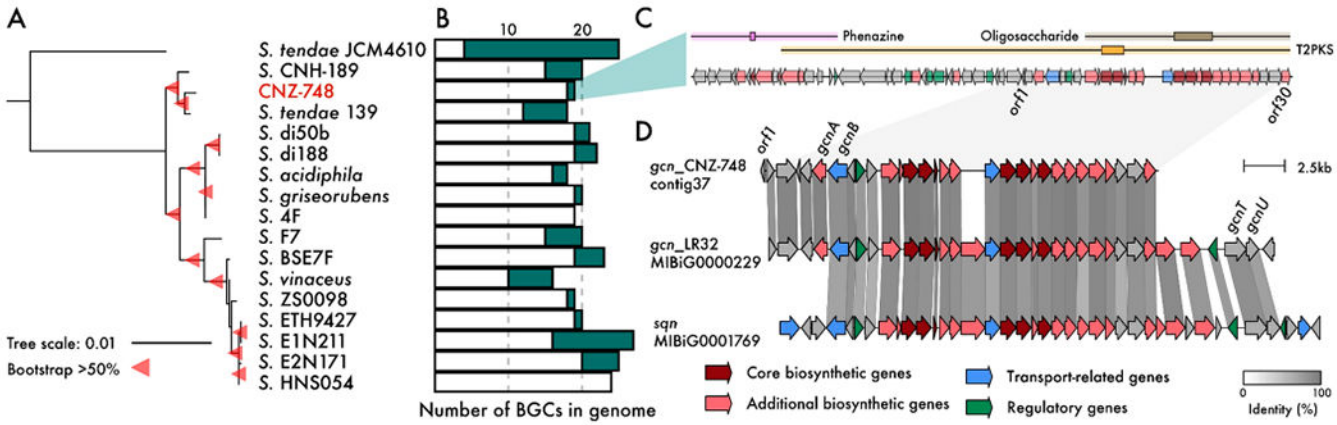

Figure 4.

Classification of CNZ-748 and analysis of the biosynthetic gene clusters (BGCs). (A) Multilocus phylogeny of 21 single-copy marker genes with the closest related genomes in the GTDB database to CNZ-748. (B) Number of BGCs detected in each genome. BGCs observed in only one strain (singletons) are highlighted in green. (C) The grincamycin (*gcn*) BGC, a type 2 PKS (T2PKS), was only observed in CNZ-748 and is the only singleton in this strain. Functional annotation of the putative essential genes (orf1–orf30) in the CNZ-748 grincamycin BGC (*gcn*-CNZ748) based on BLASTp is presented in Table S2. (D) Comparative analysis of *gcn*-CNZ748 with the grincamycin BGC from *Streptomyces lusitanus* SCSIO LR32 (*gcn*-LR32) and the saquayamycin BGC from *Streptomyces* sp. KY40–1 (*sqn*). The percentages of homology shared between genes of the BGCs are shown in greyscale.

Table 1.

^{1}H and ^{13}C NMR (CD_3OD) Data for Grincamycins P—T (1–5)

Pos.	grincamycin P (1)[a]		grincamycin Q (2)[a]		grincamycin R (3)[b]		grincamycin S (4)[b]		grincamycin T (5)[b]	
	δ_C, type[d]	δ_H, mult. (*J* in Hz)[d]	δ_C, type[d]	δ_H, mult. (*J* in Hz)[d]	δ_C, type[d]	δ_H, mult. (*J* in Hz)[d]	δ_C, type[d]	δ_H, mult. (*J* in Hz)[d]	δ_C, type[d]	δ_H, mult. (*J* in Hz)[d]
1	162.5, C		162.5, C		162.8, C		158.9, C		159.2, C	
2	136.4, C		136.5, C		137.6, C		142.8, C		143.2, C	
3	140.8, CH	7.77, d (7.8)	140.8, CH	7.76[f]	141.1, CH	7.88, d (7.8)	132.5, CH	7.38, s	132.8, CH	7.47, s
4	119.6, CH	7.81, d (7.8)	119.6, CH	7.78[f]	119.4, CH	7.81, d (7.8)	158.2, C		158.1, C	
4a	133.1, C		133.0, C		132.8, C		112.6, C		112.5, C	
5	189.6, C		189.4, C		189.7, C		192.4, C		192.2, C	
5a	116.8, C		116.7, C		116.5, C		117.0, C		116.9, C	
6	159.8, C		159.8, C		159.8, C		159.6, C		159.6, C	
7	139.4, C		139.4, C		139.3, C		139.1, C		139.1, C	
8	134.2, CH	7.92, d (7.9)	134.2, CH	7.90, d (7.8)	134.2, CH	7.93, d (7.9)	134.4, CH	7.95, d (7.8)	134.4, CH	7.94, d (7.9)
9	120.2, CH	7.86, d (7.9)	120.1, CH	7.85, d (7.8)	120.1, CH	7.89, d (7.9)	120.2, CH	7.92, d (7.8)	120.2, CH	7.91, d (7.9)
9a	133.5, C		133.4, C		133.5, C		133.8, C		133.7, C	
10	189.5, C		189.5, C		189.5, C		187.9, C		187.8, C	
10a	116.8, C		116.7, C		116.7, C		113.2, C		113.0, C	
11	41.2, CH_2	3.06, d (13.2) 3.11, d (13.2)	41.2, CH_2	3.04, d (13.3) 3.09, d (13.3)	39.4, CH_2	3.16[k] 3.45, d (13.4)	41.1, CH_2	3.00[s] 3.05[s]	39.2, CH_2	3.15[t] 3.45, br s
12	72.8, C		73.0, C		79.5, C		72.8, C		79.1, C	
13	46.9, CH_2	2.48[d] 2.51[d]	47.1, CH_2	2.44[g] 2.48[g]	50.0, CH_2	2.52, d (13.2)[m] 2.69, d (13.2)	48.1, CH_2	2.35, d (15.1) 2.39, d (15.1)	49.5, CH_2	2.57, d (13.5) 2.71, d (13.5)
14	177.1, C		177.8, C		179.0, C		180.2, C		177.8, C	
15	27.2, CH_3	1.29, s	27.2, CH_3	1.26, s	23.8, CH_3	1.44, s[L]	27.5, CH_3	1.21, s	23.7, CH_3	1.44, s
					Sugar A: D-Olivose					
1A	72.5, CH	4.91, br d (11.2)	72.5, CH	4.91[c]	72.5, CH	4.93, br d (11.6)	72.4, CH	4.94, br d (11.2)	72.4, CH	4.92, br d (11.2)
2A	40.5, CH_2	1.43, m2.50[d]	40.6, CH_2	1.42, m 2.50, m	40.5, CH_2	1.44[L] 2.51[m]	40.5, CH_2	1.43, m 2.51, m	40.5, CH_2	1.42, m 2.51, m
3A	72.6, CH	3.81, m	72.6, CH	3.80[h]	72.6, CH	3.81 (m)	72.6, CH	3.81, ddd (11.2, 8.4, 5.1)	72.6, CH	3.80, m

Pos.	grincamycin P (1)[a]		grincamycin Q (2)[a]		grincamycin R (3)[b]		grincamycin S (4)[b]		grincamycin T (5)[b]	
	δ_C, type[d]	δ_H, mult. (*J* in Hz)[d]	δ_C, type[d]	δ_H, mult. (*J* in Hz)[d]	δ_C, type[d]	δ_H, mult. (*J* in Hz)[d]	δ_C, type[d]	δ_H, mult. (*J* in Hz)[d]	δ_C, type[d]	δ_H, mult. (*J* in Hz)[d]
4A	88.0, CH	3.15, t (8.5)	87.7, CH	3.15, t (8.5)	88.0, CH	3.16[k]	88.0, CH	3.15[q]	88.0, CH	3.14[t]
5A	76.6, CH	3.57[e]	76.7, CH	3.56, m	76.6, CH	3.55 (m)	76.6, CH	3.56[r]	76.6, CH	3.57[u]
6A	18.8, CH_3	1.39, d (6.1)	18.8, CH_3	1.38, d (6.1)	18.8, CH_3	1.38, d (6.1)	18.8, CH_3	1.38, d (6.1)	18.9, CH_3	1.39, d (6.0)
					Sugar B: L-Rhodinose					
1B	100.4, CH	5.01, br s	100.2, CH	5.00, br s	100.4, CH	5.01, br s	100.4, CH	5.01, br s	100.4, CH	5.01, br s
2B	26.1, CH_2	1.66, m 2.14, m	26.0, CH_2	1.68, br d (10.9)2.07[i]	26.1, CH_2	1.68, br d (11.4)2.15[n]	26.1, CH_2	1.66, br d (12.9) 2.15, m	26.1, CH_2	1.67, br d (12.4) 2.15, m
3B	25.3, CH_2	1.87, m 2.07, m	25.2, CH_2	2.07[i] 2.12[i]	25.4, CH_2	1.86, m 2.14[n]	25.3, CH_2	1.86, m 2.06, m	25.3, CH_2	1.86, m 2.07[v]
4B	76.2, CH	3.56[e]	78.6, CH	3.76[h]	79.0, CH	3.64, br s	76.2, CH	3.56[r]	76.2, CH	3.56[u]
5B	69.2, CH	4.30, m	68.9, CH	4.38[j]	67.6, CH	4.17, m	69.2, CH	4.30, br q (6.5)	69.2, CH	4.30, br q (6.5)
6B	17.3, CH_3	1.17, d (6.5)	17.3, CH_3	1.23, d (6.5)	17.8, CH_3	1.18, d (6.6)	17.3, CH_3	1.17, d (6.5)	17.3, CH_3	1.17, d (6.5)
					Sugar C: L-Rhodinose, L-Rednose or 2-Methylthio-L-aculose					
1C	100.0, CH	4.79[c]	97.9, CH	5.22, s	99.1, CH	5.23, s	100.0, CH	4.79, d (3.4)	100.0, CH	4.74, d (3.6)
2C	30.9, CH_2	1.74, m 1.94, m	165.5, C		165.4, C		30.9, CH_2	1.74, m 1.92, m	30.9, CH_2	1.71, m 1.90, m
3C	28.5, CH_2	1.82, m	94.3, CH	5.14, s	116.8, CH	5.82, s	28.5, CH_2	1.81, m	28.5, CH_2	1.80[w]
4C	73.0, CH	3.16, m	197.3, C		195.2, C		72.8, CH	3.15[q]	72.8, CH	3.15[t]
5C	71.6, CH	3.69, m	70.8, CH	4.41[j]	71.3, CH	4.51, q (6.8)	71.5, CH	3.68, dq (6.6, 6.3)	71.5, CH	3.68, m
6C	18.2, CH_3	1.20, d (6.2)	16.9, CH_3	1.33, d (6.9)	18.5, CH_3	1.31, d (6.8)	18.2, CH_3	1.20, d (6.2)	18.2, CH_3	1.20, d (6.2)
7C					13.9, CH_3	2.41, s				
					Sugar D: L-Rhodinose					
1D					92.5, CH	5.18, br s			92.6, CH	5.20, br s
2D					26.7, CH_2	1.39, m 1.88[p]			26.8, CH_2	1.38, m 2.02[v]
3D					25.3, CH_2	1.87[p] 2.06, m			25.6, CH_2	1.78[w] 2.04[v]
4D					76.2, CH	3.56, m			76.6, CH	3.56[u]
5D					69.2, CH	4.30, qd (6.6, 1.2)			68.0, CH	4.10, br q (6.6)
6D					17.3, CH_3	1.17, d (6.6)			17.5, CH_3	1.08, d (6.5)
					Sugar E: L-Rhodinose					

Pos.	grincamycin P (1)[a]		grincamycin Q (2)[a]		grincamycin R (3)[b]		grincamycin S (4)[b]		grincamycin T (5)[b]	
	δ_C, type[d]	δ_H, mult. (*J* in Hz)[d]	δ_C, type[d]	δ_H, mult. (*J* in Hz)[d]	δ_C, type[d]	δ_H, mult. (*J* in Hz)[d]	δ_C, type[d]	δ_H, mult. (*J* in Hz)[d]	δ_C, type[d]	δ_H, mult. (*J* in Hz)[d]
1E					100.0, CH	4.79, br d (3.2)			100.0, CH	4.79, br d (3.2)
2E					30.9, CH_2	1.74, m 1.93, m			30.9, CH_2	1.71, m 1.90, m
3E					28.5, CH_2	1.78, m 1.82, m			28.5, CH_2	1.76, m 1.84, m
4E					72.8, CH	3.17[k]			72.9, CH	3.16[t]
5E					71.5, CH	3.68, m			71.4, CH	3.67, m
6E					18.2, CH_3	1.20, d (6.2)			18.2, CH_3	1.17, d (6.2)

[a] Data were acquired on a 500 MHz NMR spectrometer.

[b] Data were acquired on a 700 MHz NMR spectrometer.

[c] Overlap with residual H_2O signal.

[d] The letters d–w denote overlapping signals and assignments supported by HSQC and HMBC.

J Nat Prod. Author manuscript; available in PMC 2021 December 07.

Table 2.

Cytotoxic Activities (IC_{50}, μM) of 1–9 against PMP and Related Cancer Cell Lines

cell line	1	2	3	4	5	6	7	8	9	5-FU[a]
PMP501-1	>100	12	3.9	2.5	2.7	14	18	11	23	3.6
PMP457-2	23	>100	7.8	5.5	1.9	5.9	11	6.7	>100	2.0
ABX023-1	21	23	13	4.7	1.4	12	45	49	14	3.4
C09-1	32	17	61	10	8.7	6.6	38	42	19	4.0

[a]5-FU: 5-fluorouracil as the positive control.